MEASURING THE IMPACT OF A LANDSLIDE ON TRANSPORTATION INFRASTRUCTURE TO IMPROVE MOBILITY AND SAFETY

FINAL PROJECT REPORT

by

Margaret M. Darrow, Ph.D., P.E. and Jaimy Schwarber, E.I.T.
University of Alaska Fairbanks

Ronald P. Daanen, Ph.D.
Alaska Division of Geological & Geophysical Surveys

Sponsorship
PacTrans, Alaska Division of Geological & Geophysical Surveys, and
University of Alaska Fairbanks

for

Pacific Northwest Transportation Consortium (PacTrans)
USDOT University Transportation Center for Federal Region 10
University of Washington
More Hall 112, Box 352700
Seattle, WA 98195-2700

In cooperation with U.S. Department of Transportation,
Research and Innovative Technology Administration (RITA)

Disclaimer

The contents of this report reflect the views of the authors, who are responsible for the facts and the accuracy of the information presented herein. This document is disseminated under the sponsorship of the U.S. Department of Transportation's University Transportation Centers Program, in the interest of information exchange. The Pacific Northwest Transportation Consortium, the U.S. Government, and matching sponsor assume no liability for the contents or use thereof.

Technical Report Documentation Page

1. Report No.	2. Government Accession No.	3. Recipient's Catalog No.

4. Title and Subtitle	5. Report Date
Measuring the Impact of a Landslide on Transportation Infrastructure to Improve Mobility and Safety	October 10, 2019
	6. Performing Organization Code

7. Author(s) and Affiliations	8. Performing Organization Report No.
Margaret M. Darrow, Ph.D., P.E., University of Alaska Fairbanks ORCID 0000-0003-4078-4746 Jaimy Schwarber, E.I.T., University of Alaska Fairbanks Ronald P. Daanen, Ph.D., Alaska Division of Geological & Geophysical Surveys	

9. Performing Organization Name and Address	10. Work Unit No. (TRAIS)
PacTrans Pacific Northwest Transportation Consortium University Transportation Center for Federal Region 10 University of Washington More Hall 112 Seattle, WA 98195-2700	**11. Contract or Grant No.** 69A3551747110

12. Sponsoring Organization Name and Address	13. Type of Report and Period Covered
United States Department of Transportation Research and Innovative Technology Administration 1200 New Jersey Avenue, SE Washington, DC 20590	Final Report (Sept. 1, 2017 – Nov. 30, 2019)
	14. Sponsoring Agency Code

15. Supplementary Notes

Report uploaded to: www.pactrans.org

16. Abstract

Frozen debris lobes (FDLs) are landslides in permafrost, many located along the Dalton Highway corridor, Brooks Range, Alaska. The closest to the highway, FDL-A has demonstrated a steadily increasing rate of movement over the last several decades. Recognizing the risk, in 2018 the Alaska Department of Transportation and Public Facilities (ADOT&PF) realigned the Dalton Highway about 122 m downslope. While not a permanent solution, the realignment provided additional time for ADOT&PF to develop mitigation techniques to apply to FDLs. As part of this project, we installed subsurface geomechanical instrumentation to measure temperature and water pressure as FDL-A overrides the installation locations. We recommend continued monitoring of these installations. We successfully tested a backpack-mounted LiDAR technique, which produced high resolution (i.e., 0.1-m) digital elevation models for the FDL-A toe area. This technique allowed change detection and analysis, including volume change calculations. As of August 2, 2019, FDL-A was 17.3 m and 127.8 m from the old and new Dalton Highway embankments, respectively. Its rate of motion has transitioned from a linearly increasing rate to one that is exponential. Based on the 2019 rate, we predict that FDL-A will impact the old Dalton Highway embankment by 2021, and the new Dalton Highway by 2032. The imminent collision of FDL-A with the old embankment represents a unique opportunity to observe a landslide impacting infrastructure in a safe and controlled way and on a predictable schedule. Therefore, we recommend a Phase II portion of this research to measure the deformation of the embankment and subsurface; measure earth pressure during collision; and document the collision through geomechanical instrumentation, repeat LiDAR scans, and repeat photography.

17. Key Words	18. Distribution Statement
Frozen Debris Lobes; Landslides; Laser Radar; Embankments; Permafrost	

19. Security Classification (of this report)	20. Security Classification (of this page)	21. No. of Pages	22. Price
Unclassified.	Unclassified.	24	N/A

Form DOT F 1700.7 (8-72) Reproduction of completed page authorized.

SI* (Modern Metric) Conversion Factors

APPROXIMATE CONVERSIONS TO SI UNITS				
Symbol	**When You Know**	**Multiply By**	**To Find**	**Symbol**
		LENGTH		
in	inches	25.4	millimeters	mm
ft	feet	0.305	meters	m
yd	yards	0.914	meters	m
mi	miles	1.61	kilometers	km
		AREA		
in^2	square inches	645.2	square millimeters	mm^2
ft^2	square feet	0.093	square meters	m^2
yd^2	square yard	0.836	square meters	m^2
ac	acres	0.405	hectares	ha
mi^2	square miles	2.59	square kilometers	km^2
		VOLUME		
fl oz	fluid ounces	29.57	milliliters	mL
gal	gallons	3.785	liters	L
ft^3	cubic feet	0.028	cubic meters	m^3
yd^3	cubic yards	0.765	cubic meters	m^3
	NOTE: volumes greater than 1000 L shall be shown in m^3			
		MASS		
oz	ounces	28.35	grams	g
lb	pounds	0.454	kilograms	kg
T	short tons (2000 lb)	0.907	megagrams (or "metric ton")	Mg (or "t")
		TEMPERATURE (exact degrees)		
°F	Fahrenheit	5 (F-32)/9 or (F-32)/1.8	Celsius	°C
		ILLUMINATION		
fc	foot-candles	10.76	lux	lx
fl	foot-Lamberts	3.426	candela/m^2	cd/m^2
		FORCE and PRESSURE or STRESS		
lbf	poundforce	4.45	newtons	N
lbf/in^2	poundforce per square inch	6.89	kilopascals	kPa

APPROXIMATE CONVERSIONS FROM SI UNITS				
Symbol	**When You Know**	**Multiply By**	**To Find**	**Symbol**
		LENGTH		
mm	millimeters	0.039	inches	in
m	meters	3.28	feet	ft
m	meters	1.09	yards	yd
km	kilometers	0.621	miles	mi
		AREA		
mm^2	square millimeters	0.0016	square inches	in^2
m^2	square meters	10.764	square feet	ft^2
m^2	square meters	1.195	square yards	yd^2
ha	hectares	2.47	acres	ac
km^2	square kilometers	0.386	square miles	mi^2
		VOLUME		
mL	milliliters	0.034	fluid ounces	fl oz
L	liters	0.264	gallons	gal
m^3	cubic meters	35.314	cubic feet	ft^3
m^3	cubic meters	1.307	cubic yards	yd^3
		MASS		
g	grams	0.035	ounces	oz
kg	kilograms	2.202	pounds	lb
Mg (or "t")	megagrams (or "metric ton")	1.103	short tons (2000 lb)	T
		TEMPERATURE (exact degrees)		
°C	Celsius	1.8C+32	Fahrenheit	°F
		ILLUMINATION		
lx	lux	0.0929	foot-candles	fc
cd/m^2	candela/m^2	0.2919	foot-Lamberts	fl
		FORCE and PRESSURE or STRESS		
N	newtons	0.225	poundforce	lbf
kPa	kilopascals	0.145	poundforce per square inch	lbf/in^2

*SI is the symbol for the International System of Units. Appropriate rounding should be made to comply with Section 4 of ASTM E380.
(Revised March 2003)

Table of Contents

List of Figures

List of Tables

Acknowledgments

This research was funded by a PacTrans award, through USDOT UTC award 69A3551747110 through sub-agreement UWSC102017. The 2015 LiDAR was produced by a grant from the U.S. Department of Transportation (OASRTRS-14-H-UAF-Project B). The authors thank the Alaska Department of Transportation and Public Facilities, the Alyeska Pipeline Service Company, and the Alaska Division of Geological & Geophysical Surveys for their ongoing support.

Executive Summary

Frozen debris lobes (FDLs) are landslides in permafrost, 43 of which are located along the Dalton Highway corridor in the Brooks Range of Alaska. FDL-A, the largest and closest to the highway, has demonstrated a steadily increasing rate of movement over the last several decades. Recognizing the risk associated with FDL-A, the Alaska Department of Transportation and Public Facilities (ADOT&PF) realigned the Dalton Highway to a location about 122 m downslope of the existing alignment during the 2018 construction season. At that time, it gave ADOT&PF approximately 20 years before FDL-A would reach the new alignment. While the realignment is not a permanent solution, it provides additional time to ADOT&PF to develop appropriate mitigation techniques that can be applied to FDL-A and other FDLs in the Dalton Highway corridor. The realignment also offers the unique opportunity to measure the impacts of a landslide on transportation infrastructure. The overall objectives of this research were 1) to determine the baseline subsurface conditions between the toe of FDL-A and the highway embankment, 2) to test a backpack-mounted LiDAR system for use in change detection, and 3) to continue monitoring eight investigated FDLs.

As part of this project, we installed subsurface geomechanical instrumentation to measure temperature and water pressure. The installations are ready to be overridden by the FDL to measure the changes it induces in the subsurface. While some trends can be identified from the first year of data collection, a longer period of record will be necessary to determine the effects of FDL-A on temperature and water pressure. Therefore, we recommend continued monitoring of these installations.

The backpack-mounted LiDAR technique produced a high resolution (i.e., 0.1-m) digital elevation model for small areas. This technique allowed change detection and analysis of the FDL-A toe area, including volume change calculations and identification of areas of

sedimentation and subsequent settlement. The technique could be used in a myriad of other applications, such as assessing unstable slopes, thermokarsts affecting embankment stability, or structures such as bridges or retaining walls. As with all LiDAR collection, good weather and dust-free conditions were requirements for the LiDAR data acquisition in the backpack mode. This method, as applied to our field area, required manual cleaning of the data to scrub out vegetation and erroneous points from surface water reflections.

As of August 2, 2019, FDL-A was 17.3 m from the old Dalton Highway embankment and 127.8 m from the toe of the new Dalton Highway alignment. Its rate of motion has transitioned from a linear increase in rate to one that is exponential. As of August 2019, we predict that FDL-A will impact the old Dalton Highway embankment by 2021. At this time, it is uncertain what effect the impact with the old embankment will have on the FDL motion; however, at the measured 2019 rate, FDL-A will impact the new Dalton Highway embankment by 2032. We recommend the ongoing monitoring of FDL-A and the seven other investigated FDLs along the Dalton Highway corridor.

The imminent collision of FDL-A with the old Dalton Highway embankment represents a unique opportunity to observe a landslide impacting a roadway in a safe and controlled way and on a predictable schedule. Instrumenting the embankment will provide data on how much earth pressure a landslide applies to an engineered structure, as well as how the landslide deforms the embankment and changes the underlying permafrost. Therefore, we recommend a Phase II portion of this research in which we will 1) measure the deformation of the embankment and subsurface; 2) measure earth pressure as FDL-A collides with the embankment; and 3) document the collision through geomechanical instrumentation, repeat LiDAR scans, and repeat photography. The results from Phase II research may inform long-term mitigation efforts and

may identify an alternative solution to the FDL problem rather than repeated highway realignments.

CHAPTER 1. Introduction

The Dalton Highway (Alaska Route 11) is the only route connecting Fairbanks, Alaska, to the North Slope energy resources. The highway is instrumental in supporting the Trans Alaska Pipeline System (TAPS), which transports the oil that provides the bulk of Alaska's revenue (DeMarban 2015). Every day, between 150 and 250 tractor trailers haul needed goods and supplies to the waiting industry at its northern end and to communities and stations along the way (Stricker 2015). Hunters, tourists, and local residents also use the highway throughout the year. In 2015, major flooding along the Sagavanirktok River closed the Dalton for up to 18 days in one stretch while the flood waters receded and repairs were made (Stricker 2015). The lack of daily deliveries resulted in dramatic price increases in Deadhorse, since the supplies had to be delivered by air (DeMarban 2015). The 2015 flooding – only one example of the hazards along the highway – illustrates the impact of major shutdowns. In the words of one journalist: "The highway closure highlights the importance of Alaska's transportation infrastructure – or lack of it… (Swann 2015)."

Farther to the south in the Brooks Range, another type of hazard exists. Frozen debris lobes (FDLs) – or slow-moving landslides in permafrost – are approaching the Dalton Highway (figure 1.1). Research of these features began in earnest in 2008 with preliminary investigations of four frozen debris lobes (Daanen et al. 2012), followed by a subsurface investigation of FDL-A in 2012 (Simpson et al. 2016). In 2013, the area of interest (AOI) was expanded to include monitoring of eight FDLs (figure 1.1b). These previous investigations consisted of drilling, sampling, and installing instrumentation within FDL-A; sampling soils and rocks to determine geotechnical properties; refining geologic maps of the catchment bedrock; analyzing historic imagery to determine long-term movement rates; measuring subsurface ground temperature and displacement; measuring surface movement using a real-time kinetic global positioning system

(RTK-GPS) unit; and performing remote sensing analysis using Light Detection and Ranging (LiDAR), unmanned aerial system (UAS), and Interferometric Synthetic Aperture Radar (InSAR) data (Darrow et al. 2016, 2017; Simpson et al. 2016; Gyswyt et al. 2017; Gong et al. 2019).

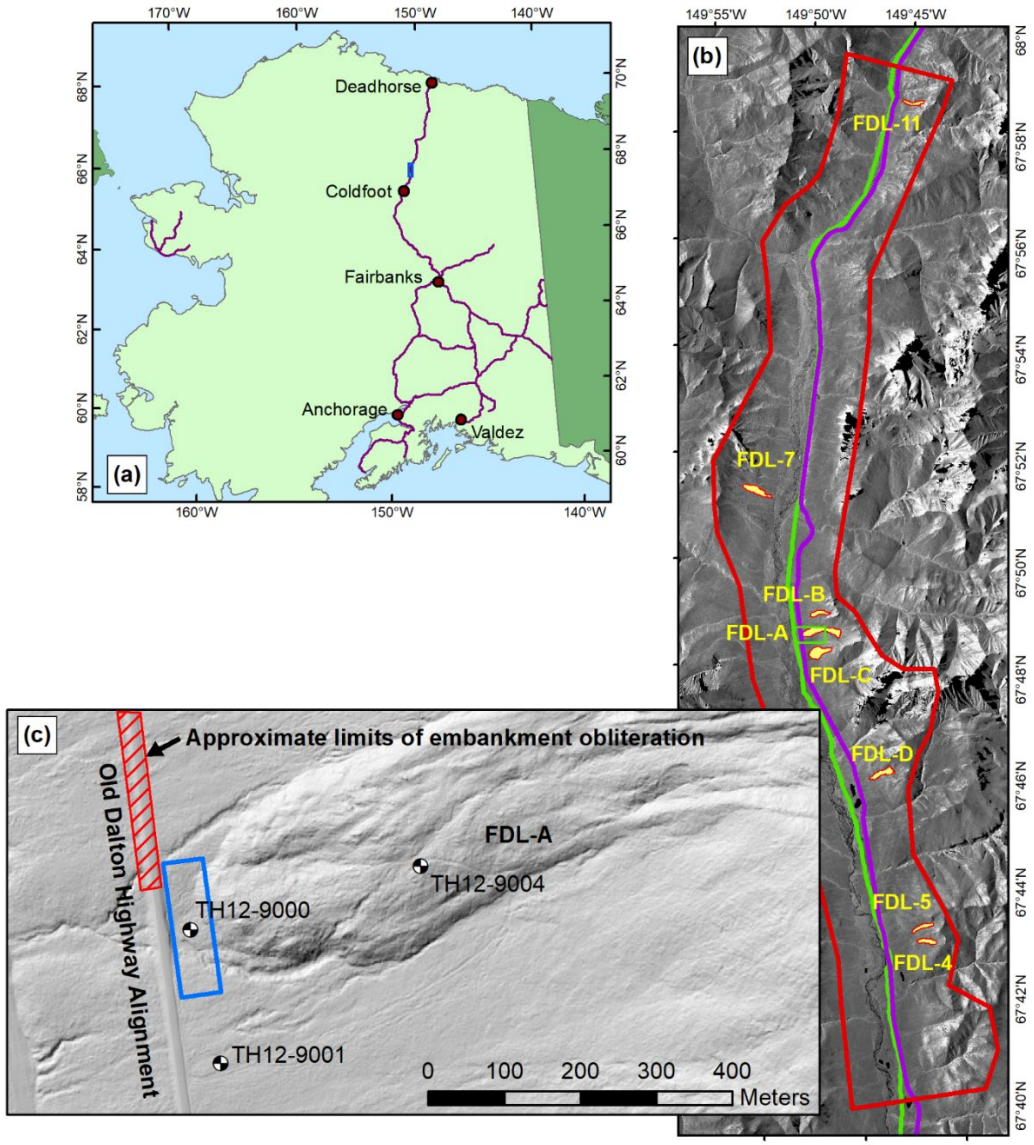

Figure 1.1. Location of project area: (a) location (shown as blue rectangle) relative to major population centers and road system; (b) area of interest (AOI; shown as red polygon) and location of eight investigated FDLs (shown in yellow); (c) FDL-A, area of 2018 instrumentation (blue rectangle), and key 2012 borings. In (b), the Dalton Highway and TAPS are shown in purple and green, respectively. Base maps data are from GINA 2001 and 2015 LiDAR (unpublished).

Recent analysis of the subsurface movement data obtained from FDL-A produced a predictive function for its surface movement (Darrow et al. 2017). Built on data collected prior to 2017, the predictive function indicated that FDL-A moved at an average rate of 4.9 m yr^{-1}, reaching a maximum velocity of 7.9 m yr^{-1} during the fall, and falling to 1.9 m yr^{-1} in the early spring. We hypothesized that the seasonal movement pattern was due to the infiltration of snow melt and the subsequent reduction of effective stress within the shear zone. Using the predictive function and the measured October 2016 distance, we predicted that FDL-A will reach the current Dalton Highway embankment in early 2023 (Darrow et al. 2017). On the basis of the annualized average rate of movement from early August 2019, however, we now predict that FDL-A will reach the highway embankment in 2021. When it reaches the highway, we estimate that *FDL-A will place ~47,000 tons of material onto the highway embankment every year* (Simpson et al. 2016). Like the 2015 flooding, *this geohazard has the potential to shut down the Dalton Highway, resulting in costly delays and increased safety concerns.*

As part of the 2012 subsurface investigation, we installed an inclinometer casing between FDL-A and the highway embankment toe (TH12-9000 in figure 1.1c). At this location, we intercepted the bedrock surface at approximately 3 m below ground surface (bgs). Unfortunately, the upper portion of this critical casing was broken at the surface sometime before June 2013. Therefore, the current analysis includes only movement since "resetting" of the inclinometer readings in August 2013 (figure 1.2). Between 2013 and 2015, movement was confined to the upper 3 m. Over the next three years, however, movement progressively penetrated deeper into the subsurface. The data collected in 2018 indicated movement as deep as 4.8 m below the surface (bgs), with a notable increase in deformation at 3 m bgs. These measurements are significant since 1) at this casing location, the bedrock surface is approximately 3 m bgs, and 2)

there is no break in slope downhill of this casing. In other words, *FDL-A is shearing deeper than the ground surface, providing enough stress in the subsurface to deform the weathered bedrock*. Unfortunately, FDL-A reached and overrode the casing location in October 2018, making future readings impossible.

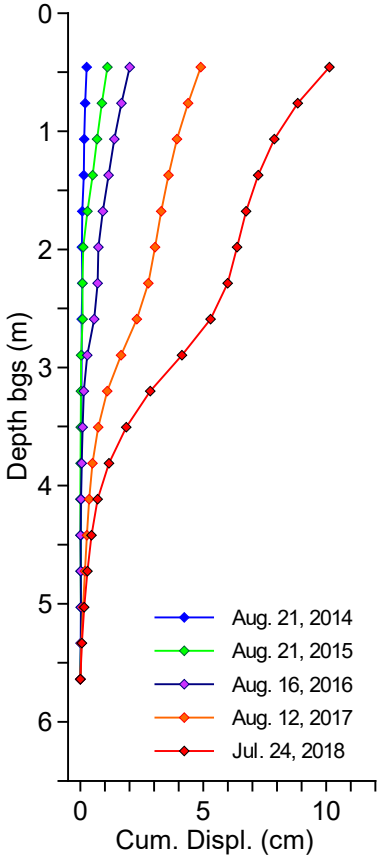

Figure 1.2. Manual inclinometer measurements of the casing installed between FDL-A and the Dalton Highway embankment (TH12-9000; see figure 1.1c for location).

Recognizing the risk associated with FDL-A, the Alaska Department of Transportation and Public Facilities (ADOT&PF) realigned the Dalton Highway to a location about 122 m downslope of the existing alignment during the 2018 construction season. While this is not a permanent solution, it provides additional time for ADOT&PF to develop appropriate mitigation techniques that can be applied to FDL-A and other FDLs in the Dalton Highway corridor. The

realignment also offers the unique opportunity to measure the impact of a landslide on transportation infrastructure. The overall objectives of the research presented herein were to determine the baseline subsurface conditions between the toe of FDL-A and the highway embankment, to test a backpack-mounted LiDAR system for use in change detection, and to continue monitoring eight investigated FDLs. Future phases of the research may include 1) measuring deformation of the embankment and subsurface; 2) measuring earth pressure during the collision of FDL-A with the embankment; and 3) documenting the collision through geomechanical instrumentation, repeat LiDAR scans, and repeat photography. Results from the future research phases may inform long-term mitigation efforts.

CHAPTER 2. Methods

For this phase of the research, we1) installed instrumentation to measure pore water pressure and temperature changes in the subsurface as the FDL approaches and covers the instrumentation locations; 2) used a backpack-mounted LiDAR system to measure FDL-A surface deformation; 3) used an RTK-GPS system to measure current the movement rates of the other seven investigated FDLs (see figure 1.1b for locations); and 4) collected data from existing automated data acquisition systems (ADAS) installed during previous field investigations. Each of these methods is discussed in more detail below.

2.1. 2018 FDL-A Instrumentation Installation

We installed the geomechanical instruments to measure changes as FDL-A approaches and covers the instrument locations, providing us with information on how FDLs modify the permafrost and pore water conditions in the subsurface ahead of them. Upon receiving the instrumentation, we calibrated the thermistors and the vibrating wire (VW) piezometers in the laboratory to ensure accurate field measurements. In July 2018, we installed a thermistor string (with sensors at 0.25, 0.5, 1, 2, and 3 m depths) and a VW piezometer at 3 m bgs in each of two boreholes located between the toe of FDL-A and the old Dalton Highway embankment (figure 2.1). The borings were advanced by using a handheld powerhead and auger (figure 2.2a). Borings TH18-01 and TH18-02 are referred to as the north and south installations, respectively. For each boring, we attached the thermistor string and VW piezometer cable to the outside of a 3-m-long PVC pipe (figures 2.2b and 2.2c). The PVC casing ensured that the sensors were installed at the correct depths, and also served as a conduit for the cement-bentonite grout with which we backfilled each boring.

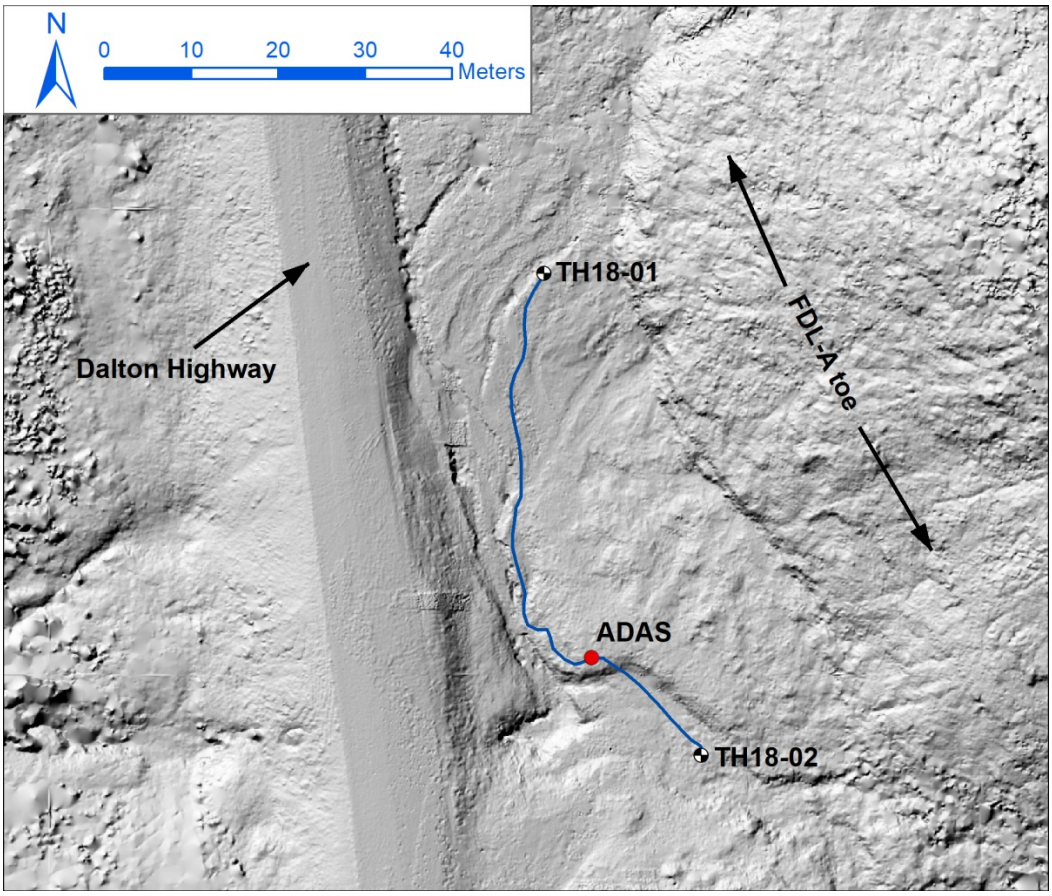

Figure 2.1. Locations of 2018 instrumentation installations. The buried cable is indicated by the dark blue curves. Background image is July 2018 LiDAR.

We routed cables from the geomechanical instrumentation to an ADAS, shallowly burying the cables to prevent damage from animals (blue curves in figure 2.1). We also installed temperature sensors to measure air and surface temperatures at the ADAS location; these readings can be used in future thermal modeling. The ADAS consisted of a 75-W solar panel, enclosure, CR1000 data logger, multiplexer, three 12-V deep cycle batteries, and a battery enclosure. This site will be referred to herein as the Dalton MP219 ADAS.

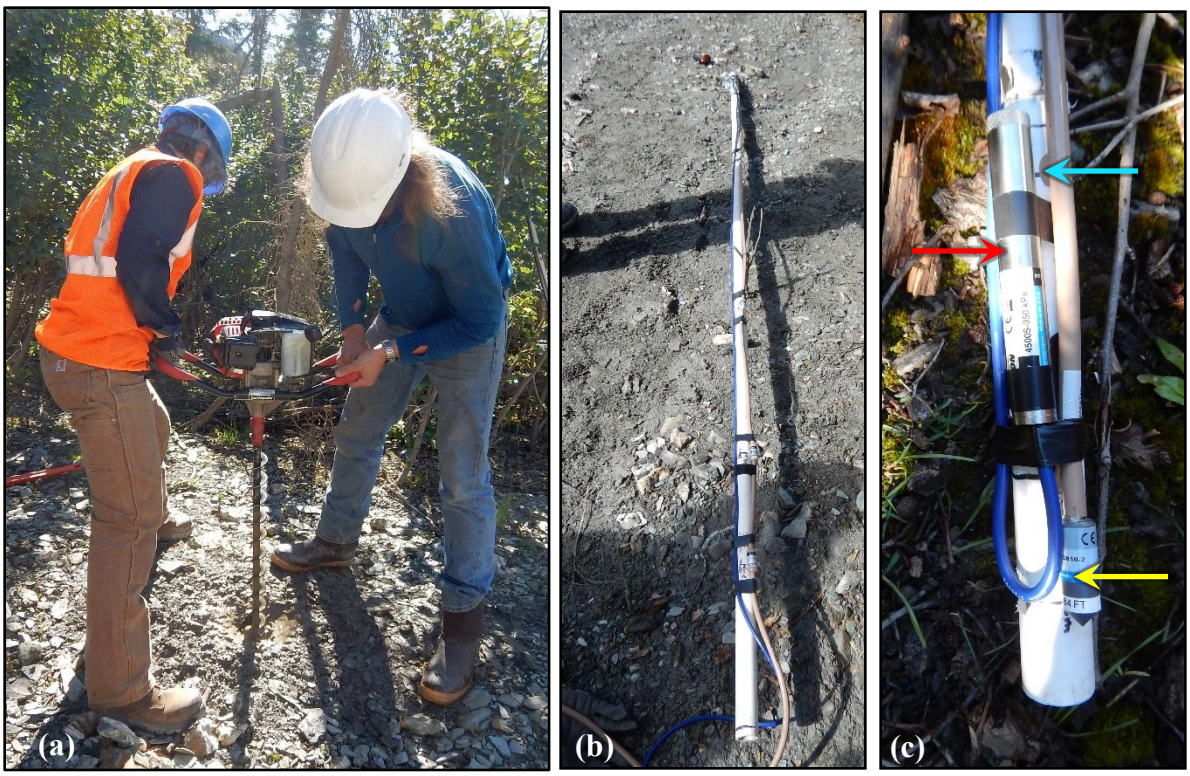

Figure 2.2. Images of the July 2018 instrumentation installation: (a) drilling with a handheld powerhead and auger; (b) instrumentation attached to a PVC casing to be inserted into the boring; (c) vibrating wire piezometer and 3.0-m-deep thermistor (indicated by red and yellow arrows, respectively) attached to the PVC casing. The blue arrow indicates the location of one of the PVC casing holes for backfilling.

As part of this current project, we collected data from two ADAS locations installed on and adjacent to FDL-A in 2012 (figure 1.1c). Since 2012, the movement of FDL-A had destroyed much of the subsurface instrumentation; however, we were still able to collect subsurface temperatures at one location on the lobe (TH12-9004), and at a location to the south of FDL-A (TH12-9001).

2.2. Backpack-Mounted LiDAR Data Acquisition

We used a backpack-mounted LiDAR system to measure surface deformation of FDL-A's toe area. LiDAR is a mobile and innovative imaging technique, from which digital elevation models (DEMs) can be produced. We used a Riegle VUX-LR integrated into a fully dynamic

LiDAR system by Phoenix LiDAR (figure 2.3). For the purpose of this study, we used a backpack to transport the LiDAR system, which allowed high-resolution scanning of a small area. The system was set up with RTK-GPS for accurate location information at 10 points per second. Between RTK-GPS readings, the system relied on a Northrop Grumman Inertial Momentum Unit (IMU) at a rate of 100 times per second. The combination of RTK-GPS and IMU devices made it possible to know the location and orientation of the LiDAR system with an accuracy of about 1 cm.

Figure 2.3. LiDAR data collection: (a) setting up the LiDAR system; (b) acquiring LiDAR data along the old Dalton Highway embankment in July 2018.

We acquired LiDAR data in July 2018, in June, and in early August 2019. Additionally, we tried to acquire a LiDAR data set when in the field in October 2018, but sub-freezing air temperatures prevented its acquisition. We used the various data sets to conduct change detection analysis of the FDL-A toe area as it approached the road, and to estimate volume change.

2.3. RTK-GPS Measurements of Eight Investigated FDLs

During the July 2018 and July /August 2019 field investigations, we completed measurements of surface marker pins on eight investigated FDLs (figure 1.1b), with an extra set of measurements of FDL-A in June 2019. We used an RTK-GPS system to make these measurements (figure 2.4), adding to a suite of measurements collected since 2012 to determine change in current movement rates of these features.

Figure 2.4. Collecting data with the RTK-GPS system in varying vegetation conditions.

CHAPTER 3. Findings

3.1. FDL-A Data Analysis

Figure 3.1 contains plots of the air and surface temperatures recorded at the Dalton MP219 ADAS from July 2018 until early August 2019. The average annual air temperature for the period of record was -2.16°C, with a minimum and maximum of -37.61°C and 32.00°C, respectively. The average soil surface temperature was 2.46°C, with a minimum and maximum of -6.31°C and 23.47°C, respectively. We calculated the *n* factors for the period of record using the air freezing and thawing indices and the surface freezing and thawing indices (Andersland and Ladanyi 2004). The final results were 0.83 for *n*-thaw and 0.21 for *n*-freeze. The low value for *n*-freeze can be explained in part by the significant snowfall recorded in the Brooks Range during the 2018-19 winter (e.g., 1.9 m in Coldfoot, Alaska (Snoflo 2019)).

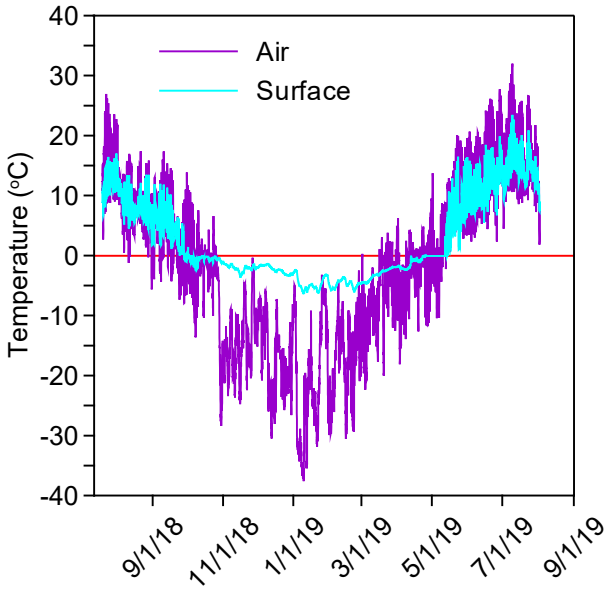

Figure 3.1. Air and surface temperatures measured at the toe of FDL-A from July 19, 2018 until August 2, 2019.

Figure 3.2 contains graphs of subsurface temperatures over time, measured by the temperature sensors installed in the two 2018 boreholes between the toe of FDL-A and the old Dalton Highway alignment. For both boreholes, temperature fluctuations attenuated with depth. The 3.0-m sensor in the north installation (figure 3.2a) demonstrated above-freezing temperatures during the summers of 2018 and 2019, indicating the absence of permafrost to a depth of at least 3.0 m, whereas the 3.0-m sensor in the south installation (figure 3.2b) remained just below freezing at -0.21°C during the entire period of record, indicating possible permafrost conditions at the south installation site. Both thermistor strings experienced some issues, with anomalous temperature spikes or drift. For example, only portions of the complete data record for the thermistors at 1.0 m and 2.0 m for the south installation are shown. We suspect that both of these thermistors may no longer be reliable and will convey this information to the vendor.

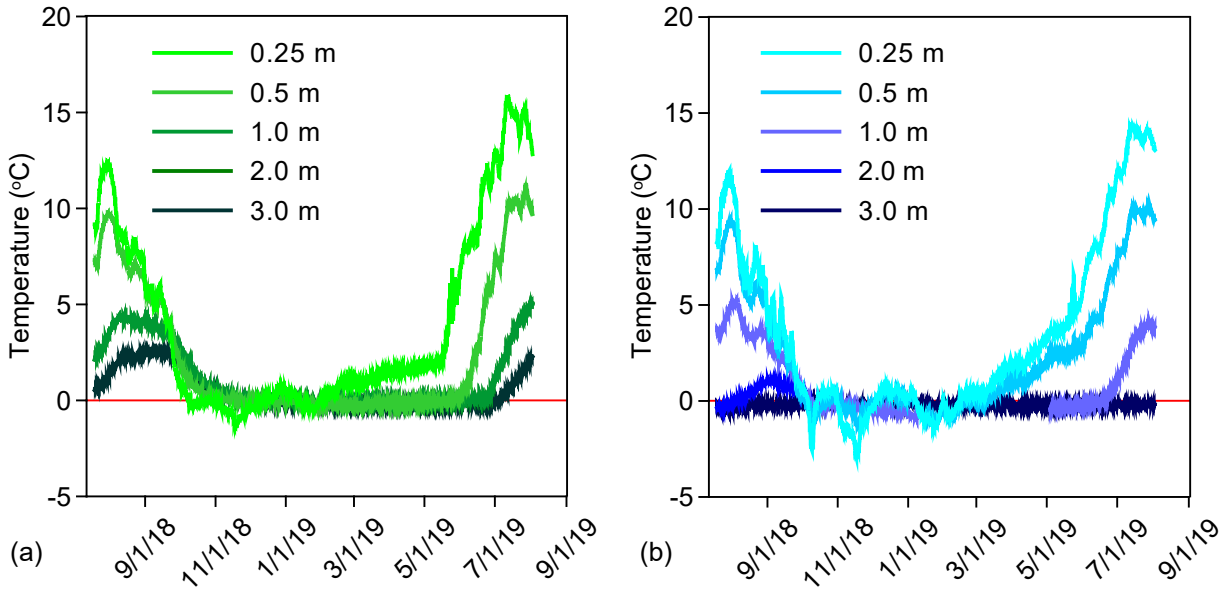

Figure 3.2. Subsurface temperatures measured in the north (a) and south (b) boreholes between the toe of FDL-A and the old Dalton Highway alignment.

Figure 3.3 contains temperature profiles for the north and south installations. Analysis of the data indicated warm conditions for the 2018-2019 measurement period, with subsurface temperatures dropping just below freezing in the winter months. Again, these warm subsurface temperatures may be explained in part by the significant snowfall during the 2018-19 winter.

Figure 3.4 contains graphs of water pressure from both installations. In the days following its installation, the south piezometer spiked to indicate ~30 m of water pressure (figure 3.4a). It is unclear whether this spike was due to the curing of the cement-bentonite grout or some other anomaly; given the fact that this spike was not recorded in the north installation, we suspect that it was an artifact of the installation and did not represent actual conditions. In figure 3.4b, the vertical axis range is limited to illustrate the data trends. Both installations measured negative pressures during the winter months, which may indicate tension due to subfreezing conditions. Both piezometers also reported a spike in water pressure during the spring snow melt period, occurring on May 7, 2019, at the south installation, and on May 18, 2019, at the north installation.

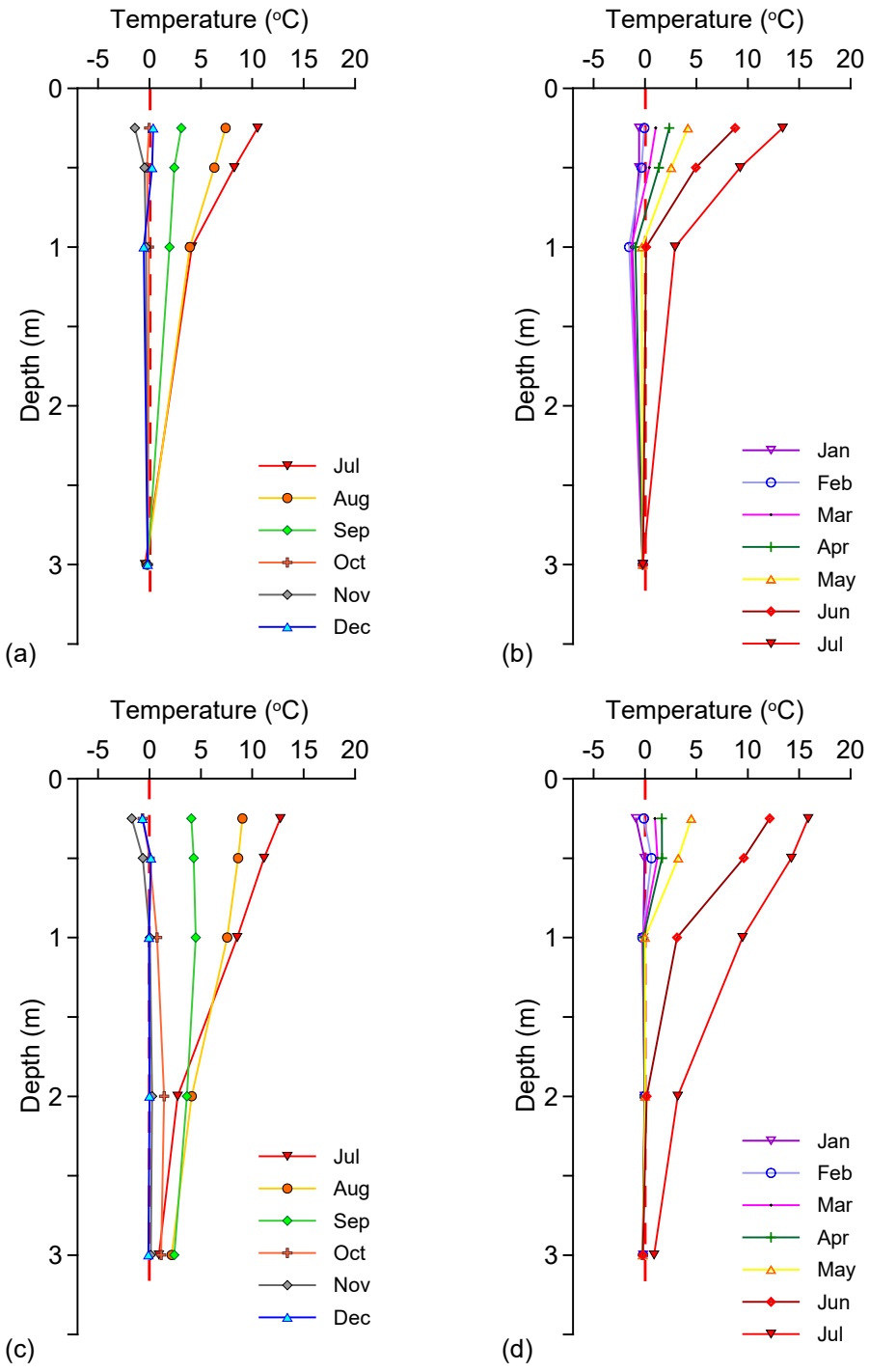

Figure 3.3. Subsurface temperatures measured near the toe of FDL-A: (a) and (b) are from the south installation (TH18-02) for 2018 and 2019, respectively; (c) and (d) are from the north installation (TH18-01) for 2018 and 2019, respectively.

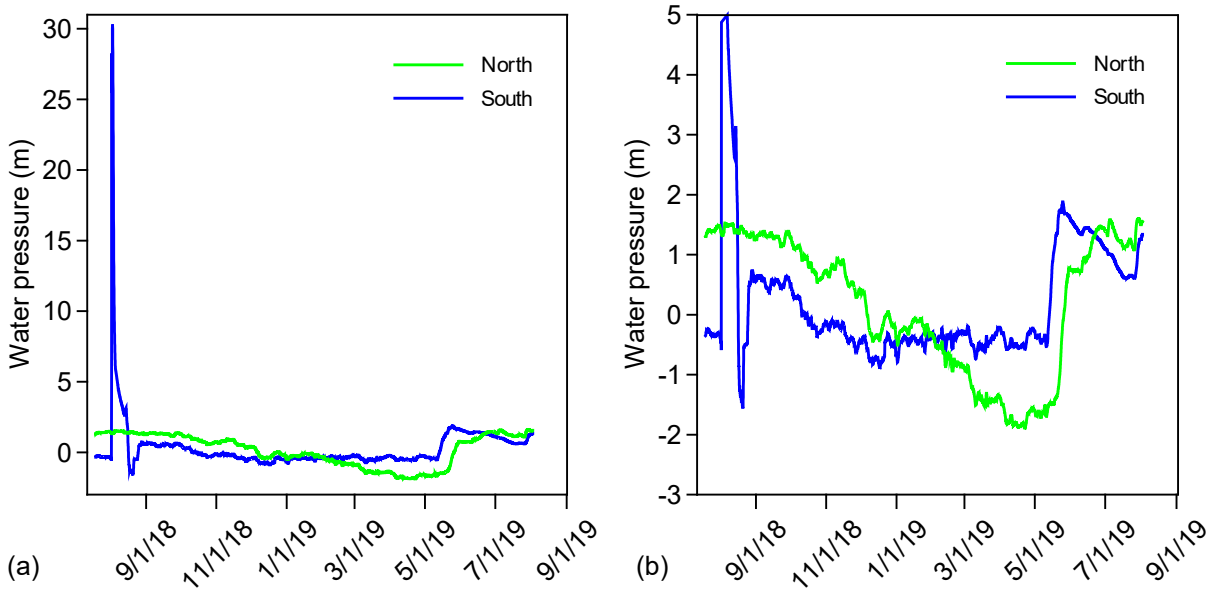

Figure 3.4. Water pressure measured near the toe of FDL-A: (a) includes all data, whereas in (b), the vertical scale has been restricted to illustrate the probable range in water pressure.

Temperature sensors at the undisturbed location south of FDL-A (TH12-9001; see figure 1.1c) were located at 0, 0.5, 1, 2, and 3 m bgs. Recorded temperatures (figure 3.5) since the fall of 2012 indicated an active layer depth between 0.5 and 1.0 m bgs; the exact depth could not be determined because of the spacing of the temperature sensors. These temperature sensors were limited to a depth of 3 m bgs, which was not deep enough to determine the temperature at the depth of zero annual amplitude. What these temperatures did record was the variation in snow fall timing and depth between 2012 and 2019. For example, in the fall of 2012, snow did not accumulate at the site until December. This lack of insulation at the surface was reflected in the cold near-surface temperatures. Years with early and deep snow accumulation (e.g., 2014 and 2018) demonstrated warm near-surface temperatures. For example, during the winter of 2018, the average monthly near-surface temperatures did not drop below -5°C.

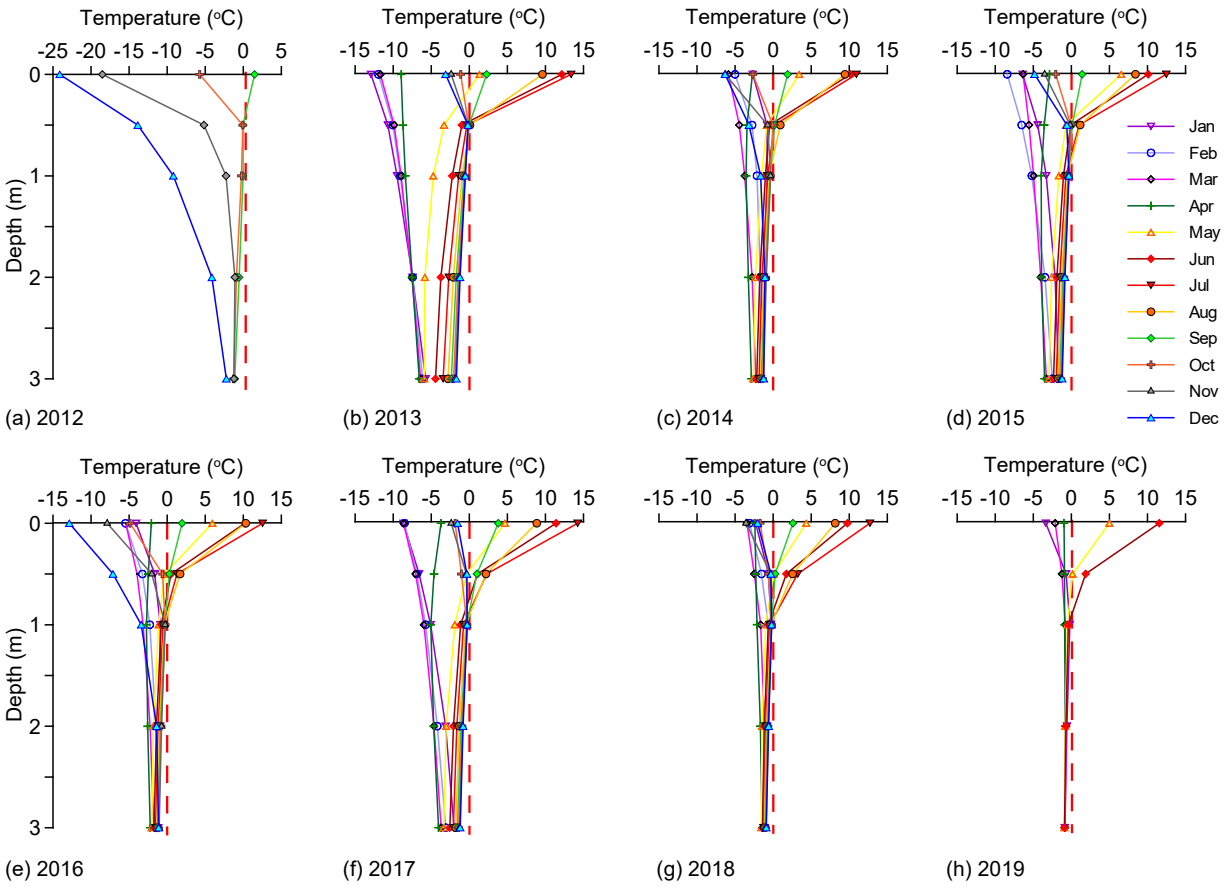

Figure 3.5. Subsurface temperature profiles from the undisturbed location south of FDL-A: (a) 2012; (b) 2013; (c) 2014; (d) 2015; (e) 2016; (f) 2017; (g) 2018; and (h) 2019. Legend for months is provided in (d). The red dashed vertical line represents the 0°C isotherm.

The subsurface temperatures and water pressure data collected in the 2018 installations represented only one year of measurements. During the July / August 2019 field work, we observed the toe of FDL-A in immediate proximity to the north installation (figure 3.6); however, at that time, neither of the installations was covered by the FDL. While some trends can be identified from the first year of data collection, a longer period of record will be necessary to determine the effects of FDL-A on temperature and water pressure. Therefore, we recommend continued monitoring of these installations.

Figure 3.6. Proximity of FDL-A's toe to the north installation on July 31, 2019. Yellow arrow indicates FDL-A toe, and blue arrow indicates position of north installation.

3.2. LiDAR Data Analysis

In general, weather affects LiDAR collection, and there is no exception for LiDAR in the backpack mode. Measuring distance with a laser through the air means that the air needs to be clear of fog, dust, rain droplets, and swarms of mosquitoes. We experienced good weather conditions during our July 2018 and June 2019 LiDAR data collection. As mentioned previously, we attempted a LiDAR data collection in October 2018, but as the air temperature was just below freezing, that attempt was unsuccessful. The instrument has a temperature range limitation (0°C to 40°C) to protect the integrity of the moving mirror. In August 2019, we acquired the LiDAR data in between rain showers, which resulted in less optimal data and more manual corrections because of laser reflections from water droplets on the wet vegetation.

After collecting the raw LiDAR data, we scrubbed the data to remove laser returns from trees and shrubs, as well as erroneous points caused by reflection from surface water. Figure 3.7a is the 2015 1-m resolution LiDAR data for the study area, with the 2015 FDL-A toe area

indicated by the blue shading. Typically, we do not have a new LiDAR data set when conducting field work, so we measure the toe location of each FDL by using the RTK-GPS system (FDL-A's July 2018 position is indicated by the red line in figure 3.7a). With the back-pack mounted LiDAR system, *we produced 0.1-m resolution DEM of FDL-A's toe area*, allowing a more thorough analysis of this critical infrastructure area. Hillshades produced from the July 2018, June 2019, and August 2019 DEMs are overlaid on the 2015 LiDAR data in figures 3.7b, 3.7c, and 3.7d, respectively. There are some artifacts present in the June 2019 data set, visible as horizontal lines. These are due to a combination of lack of RTK during the field work and manual post-processing steps. Despite the artifacts, the backpack-mounted LiDAR system proved a success, producing DEMs with 0.1-m accuracy that allow for the detection and analysis of surface morphology changes.

Figure 3.8 consists of three longitudinal profiles of the toe of FDL-A constructed along the double arrow black line indicated in figure 3.7b, and derived from the three different DEMs produced with the backpack-mounted LiDAR. The yearly change between July 2018 and August 2019 is most noticeable, with the forward motion of FDL-A resulting in a reduction in distance to the old Dalton Highway embankment. The seasonal change from June to August 2019 is not as significant, although the forward motion is still evident at the bottom of the slope. Another change that is notable is the increase in elevation of the ground surface between the FDL toe and the highway embankment between 2018 and 2019. This is due to sediment deposition along a creek that drains FDL-A and crosses under the highway embankment through several culverts.

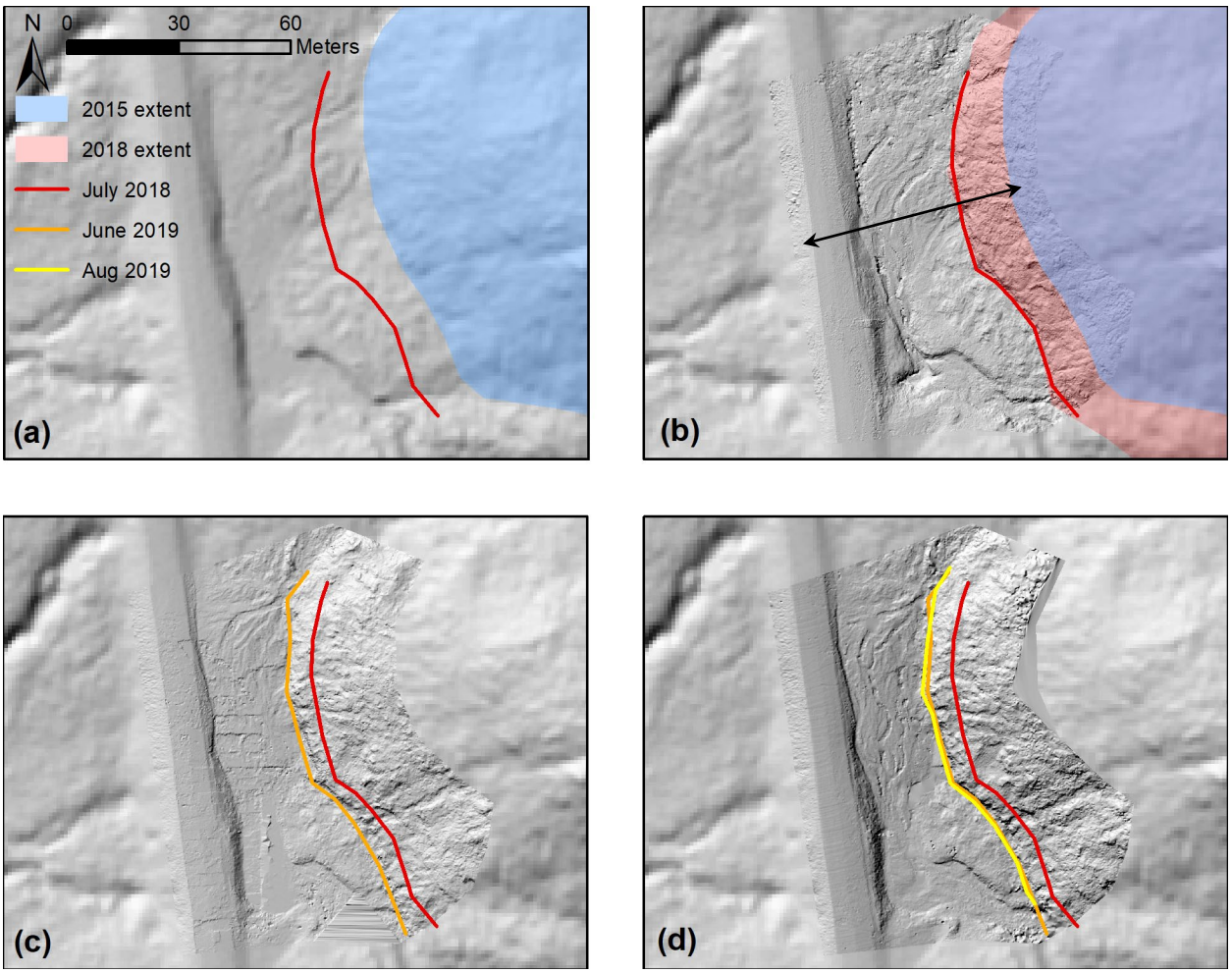

Figure 3.7. LiDAR data set comparison. The background image in all sub-figures is 1-m resolution 2015 LiDAR. In (b) – (d), the background is a combination of the 2015 LiDAR and the July 2018, June 2019, and August 2019 LiDAR data sets, respectively. The double arrow black line is the location of the longitudinal profiles included in Figure 3.8. The legend elements displayed in (a) apply to all sub-figures.

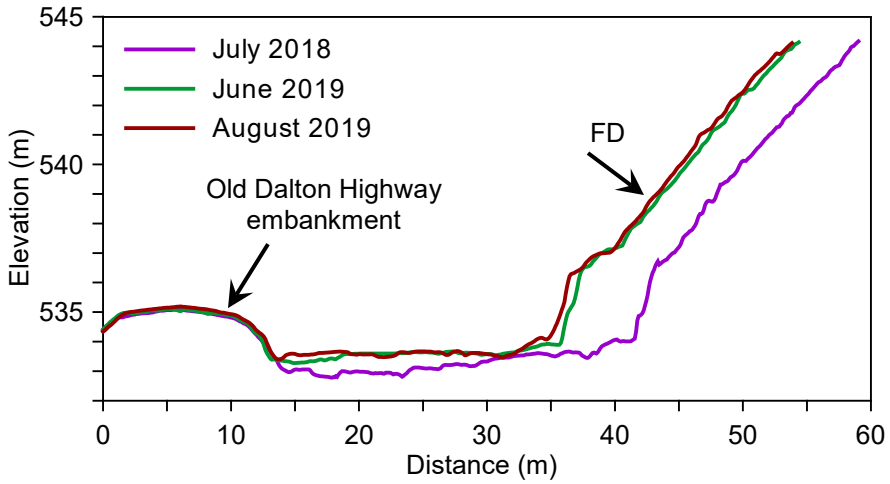

Figure 3.8. Longitudinal profiles of the toe of FDL-A generated from LiDAR DEMs from 2018 and 2019.

While the longitudinal profiles provide a view of temporal changes, these changes are specific to the selected profile line. Analysis of the full DEMs allows for a more comprehensive comparison. For example, DEMs of similar extent and resolution can be differenced, which allows for qualitative analysis of the surface and quantitative volume change calculations. Figure 3.9 provides examples of DEMs of Difference (DoD) illustrating yearly changes (i.e., between July 2018 and August 2019 in figure 3.9a) and seasonal changes (i.e., between June and August 2019 in Figure 3.9b). Because the integrated error of a single data set using the backpack mode was approximately 0.1 m, we masked all values that were 0 m ± 0.1 m within each DoD. Over one year, the most significant change was the advance of FDL-A's toe. Observation of the color-contoured zones in figure 3.9a provides a quick indication of which part of the toe is most active (i.e., the dark green zone (indicated by red arrow) representing 3 to 6 m of vertical change). The stream area between FDL-A's toe and the old highway alignment experienced sediment deposition, with the area upstream of a culvert completely filling in over the year (indicated by the blue arrow in figure 3.9a). We also observed this sedimentation over the life of

this project. For example, in October 2018 we observed an approximately 1.5-m high bank to the stream channel between the highway embankment and the ADAS location (figure 3.10a). During the winter, some ice formed near the culvert inlet. By the next summer, this stream channel had been completely filled with sediment, and the culvert inlet and adjacent ice were buried (red arrow in figure 3.10b).

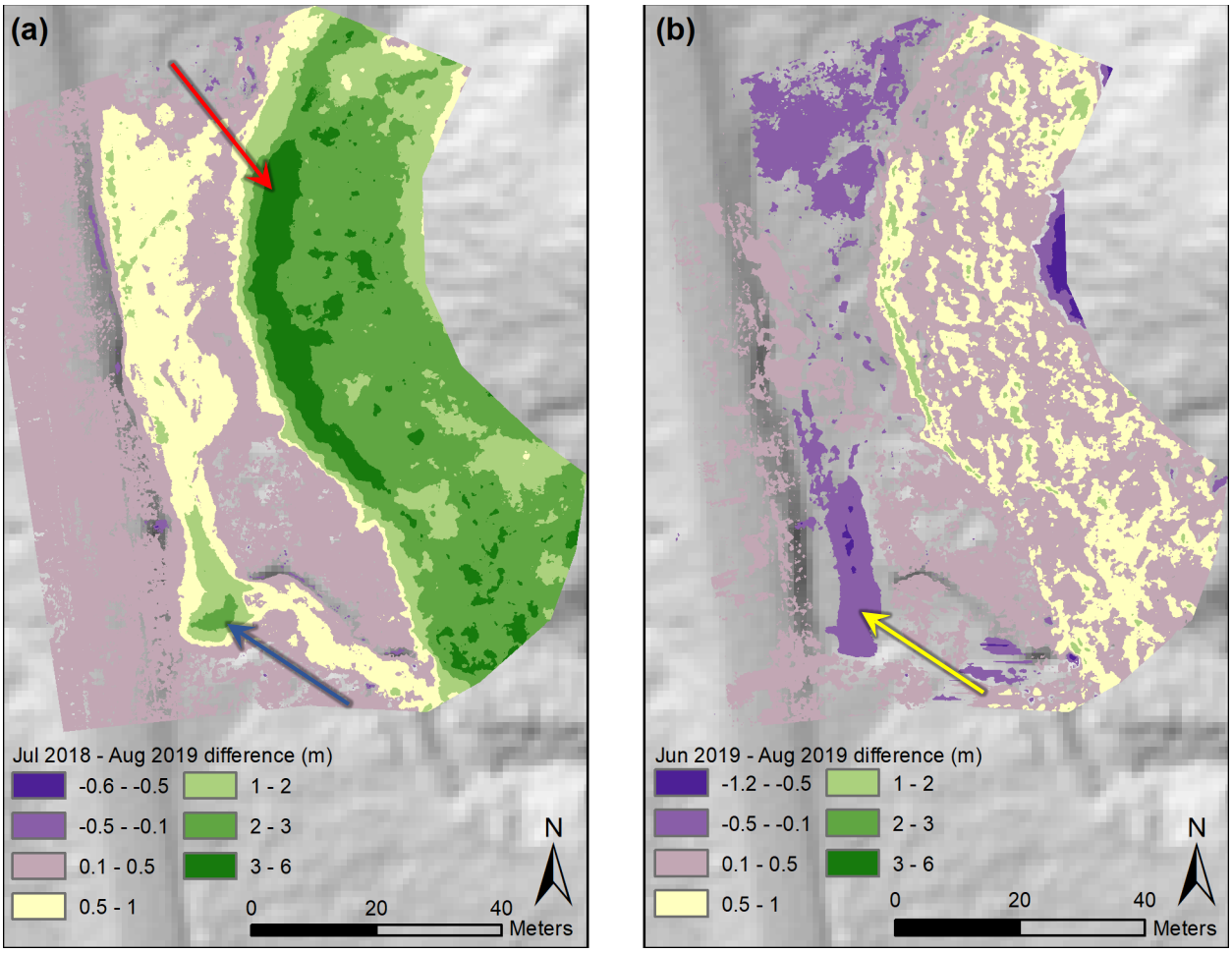

Figure 3.9. DEMs of Difference (DoD) for (a) yearly changes (July 2018 to August 2019), and (b) seasonal changes (June 2019 to August 2019). Background image is 2015 LiDAR.

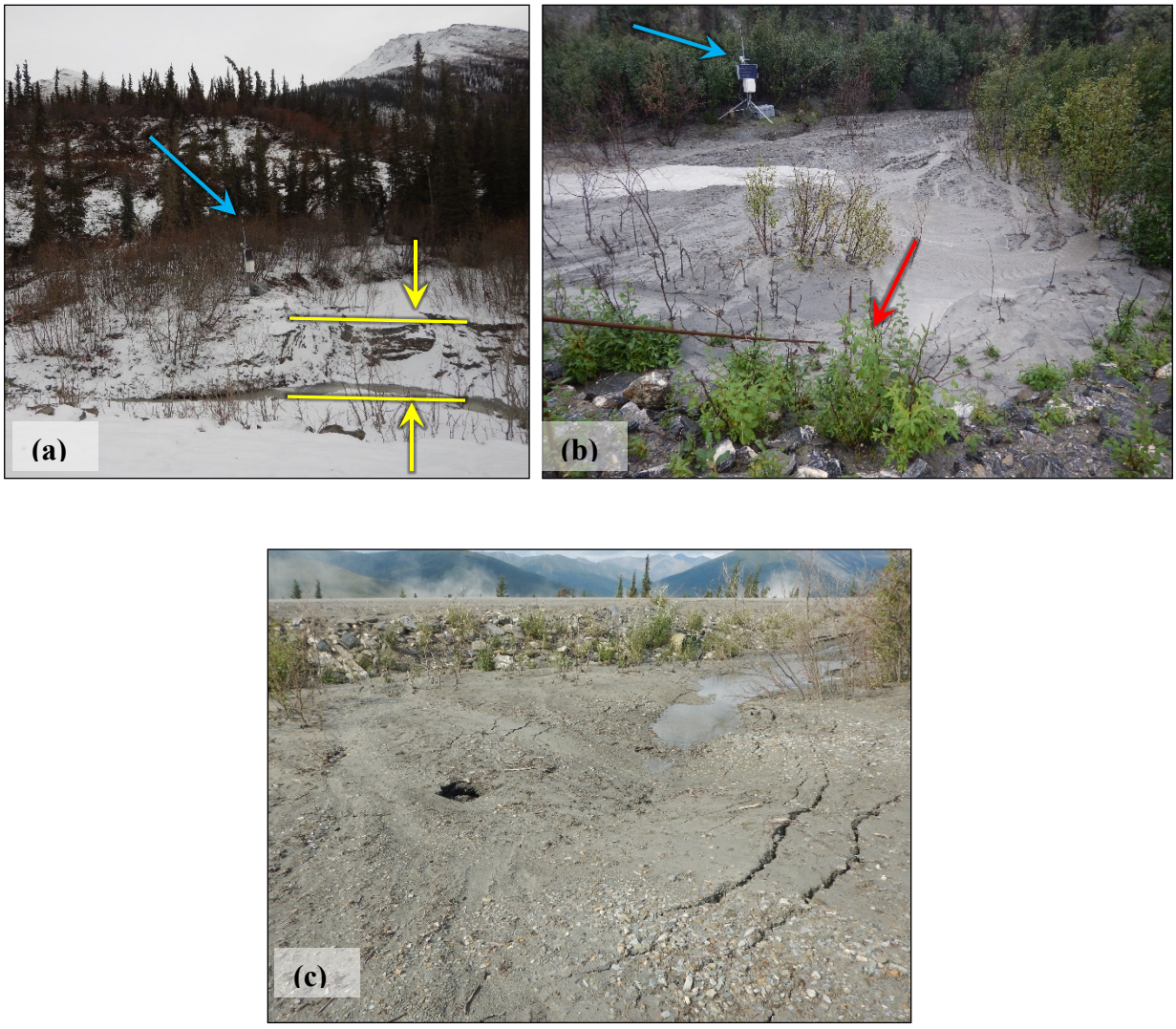

Figure 3.10. Photographs illustrating changes in sedimentation between the toe of FDL-A and the old Dalton Highway embankment. (a) Looking east towards the south flank of FDL-A from the highway embankment on October 13, 2018. The blue arrow indicates the Dalton MP219 ADAS, and the yellow lines and arrows indicate a steep drop of about 1.5 m into the stream channel. (b) Similar view on August 3, 2019, with the blue arrow indicating the ADAS location and the red arrow indicating the location of a buried culvert inlet. (c) Looking west towards the highway embankment on July 31, 2019. The buried culvert inlet is to the left of the photograph.

Over the summer of 2019, the nature of the change in the area was different. The entire lobe front demonstrated advancement over the summer months, and the same area of the FDL toe remained the most active, demonstrating up to 2 m of vertical change (figure 3.9b). The seasonal changes suggested areas of oversteepening along the toe slope, although the overall

slope angle remained similar (figure 3.8). The seasonal changes also indicated that the area of sedimentation in front of the culvert experienced some settlement during the summer (see yellow arrow in figure 3.9b). The settlement was visually evident in the field, as manifested by tension cracks, ponding, and holes (figure 3.10c). This settlement may have been due in part to the melting of the ice that formed during the preceding winter and was subsequently buried by sediment.

We used the DoD for the July 2018 – August 2019 period to calculate change in volume of the toe region of FDL-A and the amount of sediment deposited between the FDL toe and the toe of the old highway embankment; table 2.1 contains a summary of the relevant parameters. Over the one-year period, 7.46×10^3 m^3 of debris advanced downslope in the toe region of FDL-A. It must be stressed that this is only in the area measured, which was limited by passable conditions in the field. For example, we were not able to survey the upper portion of the toe slope because of dense vegetation. Also, the area surveyed was only the most-downslope portion of FDL-A, and did not represent its complete width. Therefore, the volume change presented in table 2.1 should not be used in volume per unit width calculations. Between the toe of FDL-A and the toe of the old Dalton Highway embankment, approximately 1.28×10^3 m^3 of sediment were deposited during the period of study. This volume calculation also includes the ice that formed over the winter and was buried by sediment.

Table 2.1 Summary of volume calculations for the toe area of FDL-A between July 2018 and August 2019

Property	**FDL-A toe**	**Area between FDL-A toe and Dalton Highway embankment**
Area (m^2)	3,184	2,780
Volume change (m^3)	7,455	1,282
Average change in elevation (m)	2.34	0.46

The LiDAR DEMs were complementary to our yearly RTK-GPS measurements of FDL-A's toe position, providing a more comprehensive view of surface morphology changes. *As of August 2, 2019, FDL-A was 17.3 m from the old Dalton Highway embankment, and 127.8 m from the toe of the new Dalton Highway alignment* (figure 3.11).

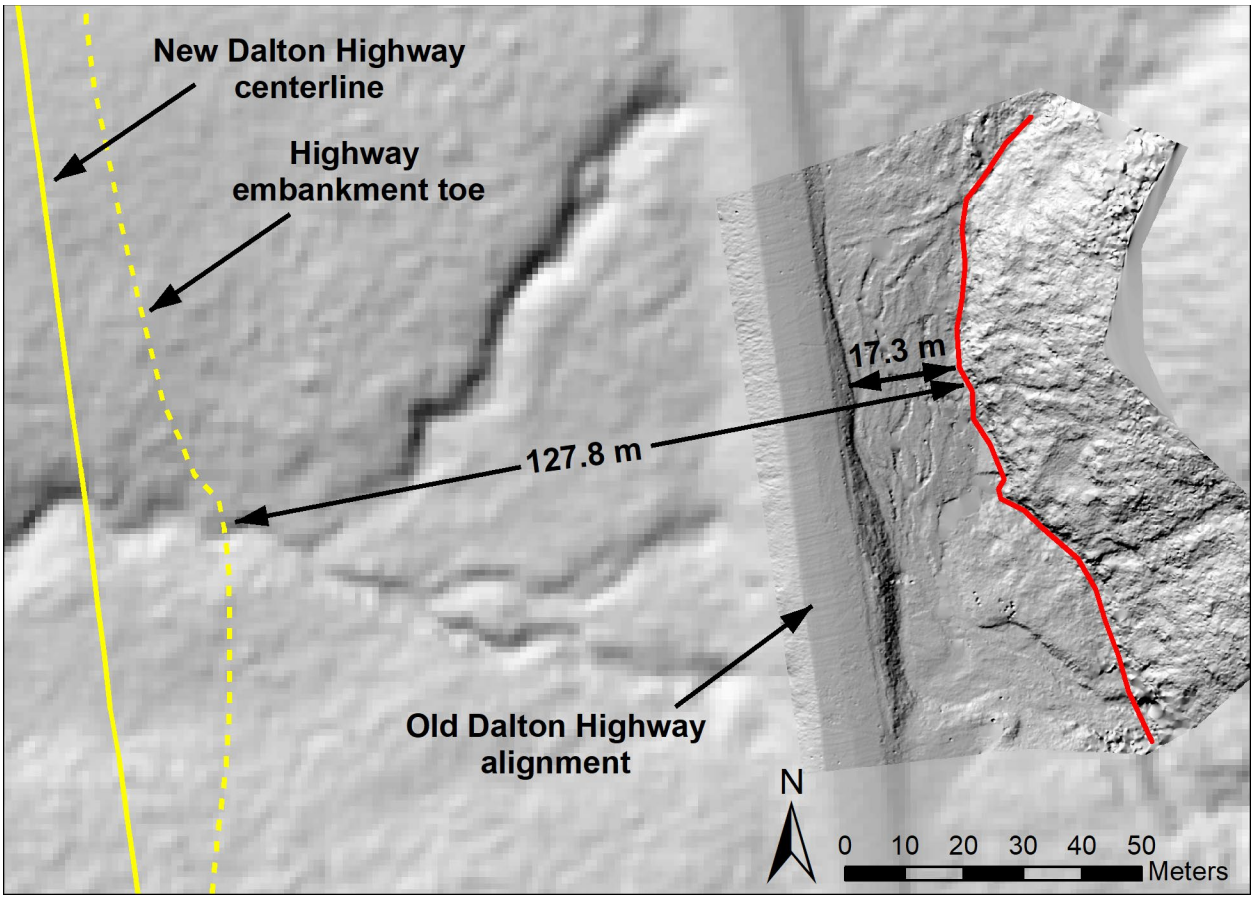

Figure 3.11. Location of FDL-A relative to the old and new Dalton Highway embankments as of August 2, 2019. Background image is a combination of August 2018 LiDAR (0.1-m resolution) and 2015 LiDAR (1-m resolution).

3.3. FDL Rates of Movement

As a part of ongoing monitoring efforts, we measured the locations of surface marker pins across the surfaces of FDL-A and seven other FDLs in the area of interest by using an RTK-

GPS system. Figure 3.12 is a graphical representation of the annualized rates of movement for each of the eight monitored FDLs, including lines representing long-term trends. *Overall, the continuing long-term trend for the monitored FDLs is an increasing rate of movement*. Several of the monitoring points on the lower portions of FDL-7 and FDL-D were covered by debris or fell into cracks on these rapidly-moving lobes, and thus were lost. Because the rates presented are an average of all monitored points, losing points in the fastest moving sections will affect the perceived rate of motion, effectively lowering the rate. As part of the July / August 2019 field work, we replaced three surface marker pins on each of these lobes.

As indicated in the Introduction, we developed a predictive function to quantify the movement of FDL-A. This predictive function is based partly on a linear increase of FDL-A's rate of movement as determined from historic imagery (blue dashed line in figure 3.13). When current movement rates based on RTK-GPS measurements are included, however, the goodness of fit of the linear function is reduced (orange dashed line in figure 3.13). Instead of a linear function, *the best fit has become exponential* (red curve in figure 3.13). The current movement rates of several other FDLs also can be explained in a similar fashion. In 2018, the ADOT&PF completed the realignment of the Dalton Highway in front of FDL-A (figure 3.14), effectively "buying" 20 years of time before FDL-A impacts the new alignment location. On the basis of our 2019 measurements – only one year later – *the cushion of time has been reduced to only 13 years*.

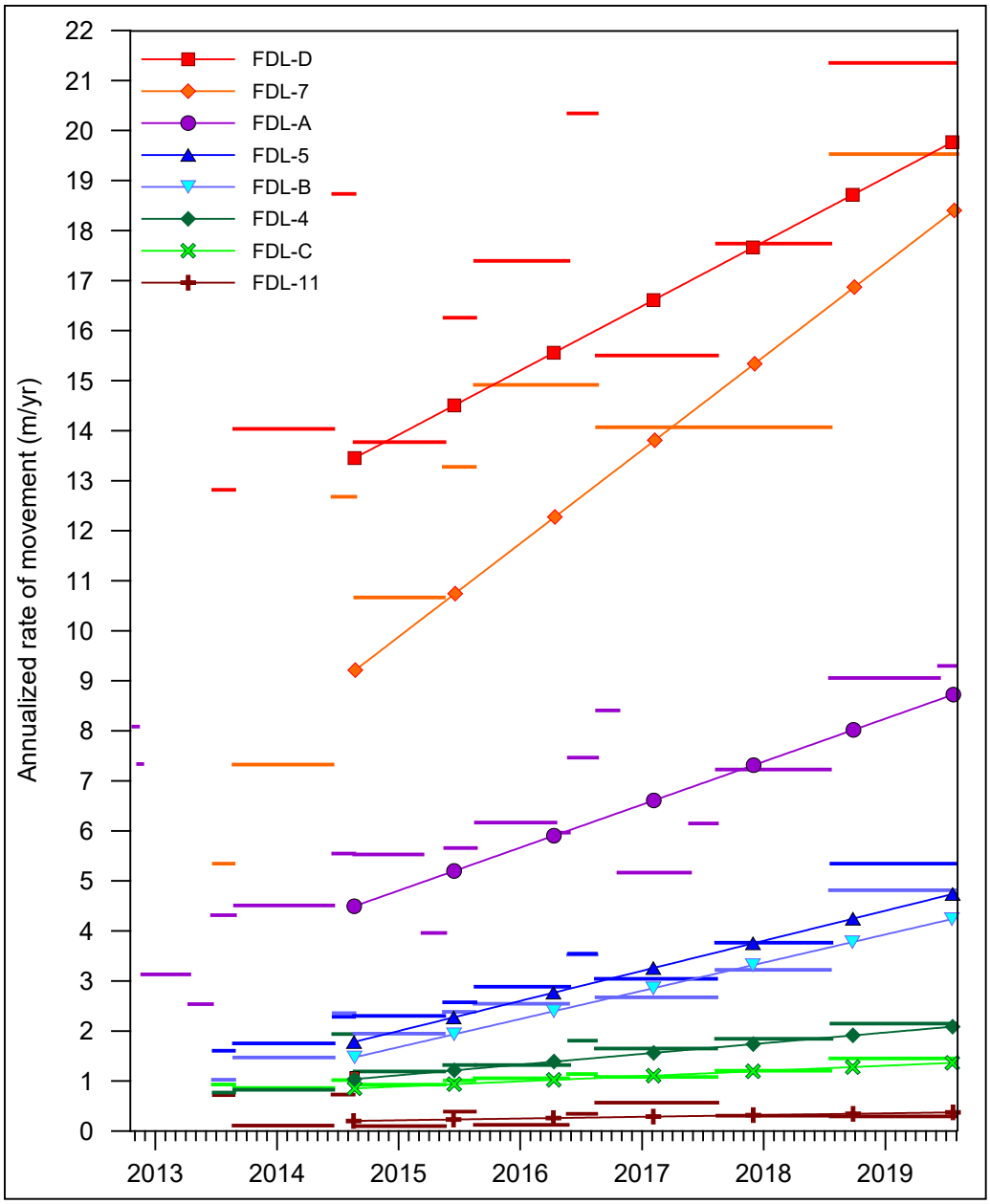

Figure 3.12. Annualized rate of movement summary for the eight investigated FDLs from late 2012 (for FDL-A) to July / August 2019.

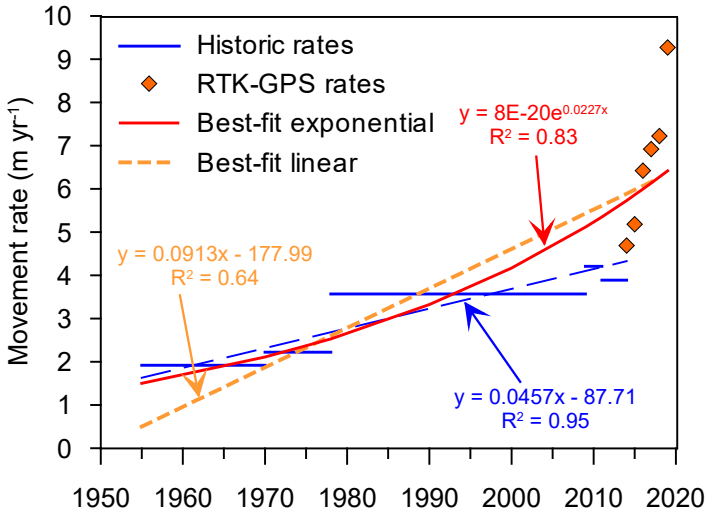

Figure 3.13. FDL-A's increasing rate of movement since 1955.

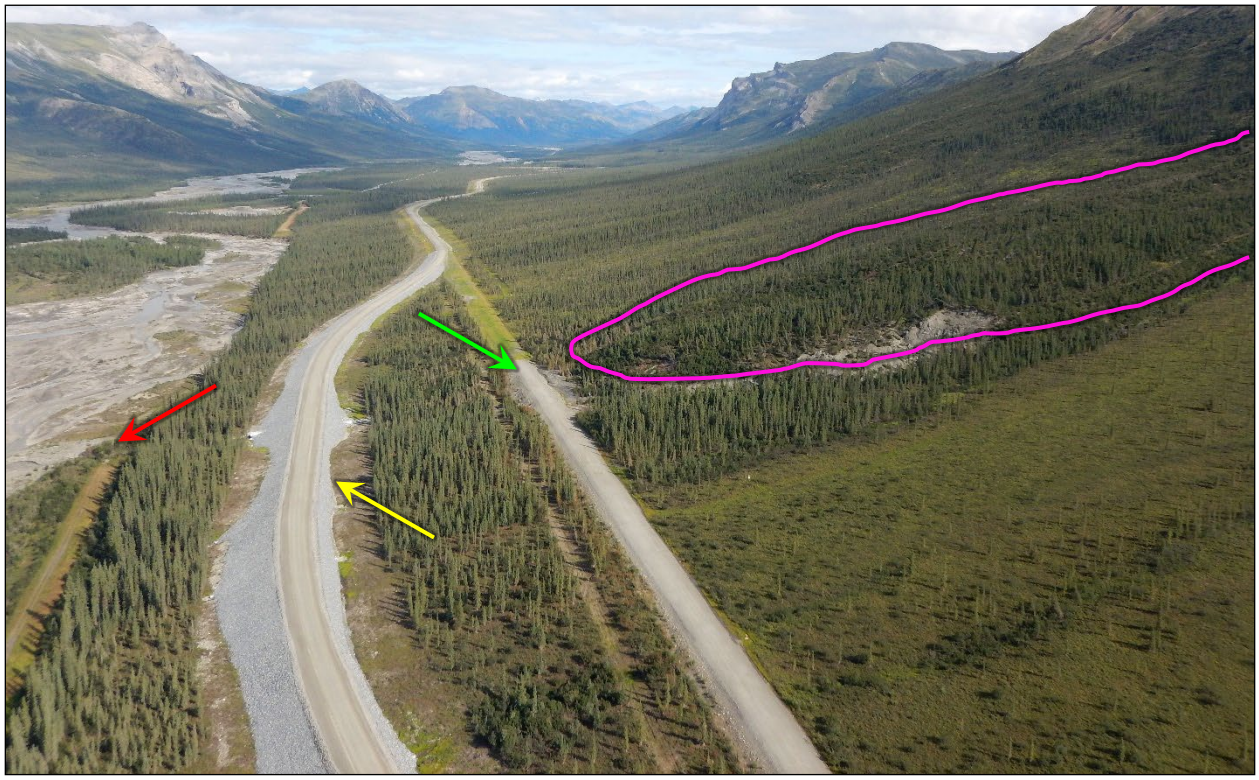

Figure 3.14. Oblique view of FDL-A (outlined in pink), the old (green arrow) and new Dalton Highway (yellow arrow) alignments, and the location of the buried Trans Alaska Pipeline System (red arrow), as seen in August 2019.

CHAPTER 4. Conclusions

Over the life of this project, we 1) successfully installed and monitored geomechanical instrumentation located between the toe of FDL-A and the toe of the old Dalton Highway embankment; 2) successfully tested a backpack-mounted LiDAR system for use in change detection; and 3) continued to monitor eight investigated FDLs to determine their ongoing rates of movement. The following summarizes our observations and recommendations:

- Subsurface devices measuring temperature and water pressure are in place adjacent to the toe of FDL-A and ready to be overridden by the FDL to measure the changes it induces in the subsurface. While some trends can be identified from the first year of data collection, a longer period of record is necessary to determine the effects of FDL-A on temperature and water pressure. Therefore, we recommend continued monitoring of these installations.
- The backpack-mounted LiDAR technique produced a high resolution (i.e., 0.1 m) digital elevation model for small areas. This technique allowed change detection and analysis of the FDL-A toe area, including volume change calculations and identification of areas of sedimentation and subsequent settlement. The technique could be used in a myriad of other applications, such as assessing unstable slopes, thermokarsts affecting embankment stability, or structures such as bridges or retaining walls. As with all LiDAR collection, good weather and dust-free conditions are requirements for the LiDAR data acquisition in the backpack mode. This method, as applied to our field area, required manual cleaning of the data to scrub out vegetation and erroneous points from surface water reflections.
- As of August 2, 2019, FDL-A was 17.3 m from the old Dalton Highway embankment, and 127.8 m from the toe of the new Dalton Highway alignment. Its rate of motion has

transitioned from a linear increase in rate to one that is exponential. As of August 2019, we predict that FDL-A will impact the old Dalton Highway embankment by 2021. At this time, it is uncertain what effect the impact with the old embankment will have on the FDL motion; however, at the measured 2019 rate, FDL-A will impact the new Dalton Highway embankment by 2032. We recommend the ongoing monitoring of FDL-A and the seven other investigated FDLs along the Dalton Highway corridor.

- The imminent collision of FDL-A with the old Dalton Highway embankment represents a unique opportunity to observe a landslide impacting a roadway in a safe and controlled way and on a predictable schedule. Instrumenting the embankment will provide data on how much earth pressure a landslide applies to an engineered structure, and how the landslide deforms the embankment and changes the underlying permafrost. Therefore, we recommend a Phase II portion of this research in which we will 1) measure the deformation of the embankment and subsurface; 2) measure earth pressure as FDL-A collides with the embankment; and 3) document the collision through geomechanical instrumentation, repeat LiDAR scans, and repeat photography. The results from Phase II research may inform long-term mitigation efforts and may identify a solution to the FDL problem other than repeated highway realignments.

REFERENCES

Andersland, O. B. and Ladanyi, B. (2004). *Frozen Ground Engineering*, 2nd Ed.: John Wiley & Sons, Inc., Hoboken, NJ, 363 p.

Daanen, R. P., Grosse, G., Darrow, M. M., Hamilton, T. D., Jones, B. M. (2012). "Rapid movement of frozen debris-lobes: implications for permafrost degradation and slope instability in the south-central Brooks Range, Alaska." *Natural Hazards and Earth System Science:* 12, 1521-1537, doi:10.5194/nhess-12-1521-2012

Darrow, M. M., Gyswyt, N. L., Simpson, J. M., Daanen, R. P., Hubbard, T. D. (2016). "Frozen debris lobe morphology and movement: an overview of eight dynamic features, southern Brooks Range, Alaska." *The Cryosphere*: 10, 977-993, doi:10.5194/tc-10-977-2016

Darrow, M. M., Meyer, F., Cunningham, K. W., Gong, W., Gyswyt, N. L., McCoy, R. P., Daanen, R. P., McAlpin, D. (2017). *Monitoring and Analysis of Frozen Debris Lobes Using Remote Sensing, OASRTRS-14-H-UAF-B, Final Report*: Institute of Northern Engineering, UAF, Fairbanks, Alaska, 107 p.

Darrow, M. M., Daanen, R. D., Gong, W. (2017). "Predicting movement using internal deformation dynamics of a landslide in permafrost." *Cold Region Science and Technology*: 143, 93-104, https://doi.org/10.1016/j.coldregions.2017.09.002

DeMarban, A. (2015). " 'Epic' flooding on Dalton Highway hinders North Slope oil operations." *Alaska Dispatch News*, accessed August 8, 2017, https://www.adn.com/environment/article/epic-flooding-north-slope-oil-finds-hindering-daily-operations/2015/05/22/

GINA – Geographic Information Network of Alaska. (2001). *Interferometric Synthetic Aperture Radar (IfSAR)*: http://www.gina.alaska.edu/data/ifsar (last access: 9 December 2015).

Gong, W., Meyer, F. J., Darrow, M. M., Daanen, R. P. (2019). "Reconstructing movement history of frozen debris lobes in northern Alaska using satellite radar interferometry." *Remote Sensing of Environment*: 221, 722-740.

Gyswyt, N. L., Darrow, M. M., Daanen, R. P. (2017). "Using LiDAR to analyze mass movement of frozen debris lobes, Brooks Range, Alaska." *3rd North American Symposium on Landslides, June 4-8, 2017:* Roanoke, VA.

Mao, J. (2005). "A finite element approach to solve contact problems in geotechnical engineering." *International Journal for Numerical and Analytical Methods in Geomechanics*: 29, 525-550, doi:10.1002/nag.424

Simpson, J. M., Darrow, M. M., Huang, S. L., Daanen, R. P., Hubbard, T. D. (2016). "Investigating movement and characteristics of a frozen debris lobe, south-central Brooks Range, Alaska." *Environmental and Engineering Geoscience*: 22(3), 259-277.

Snoflo. (2019). "Snow Report Coldfoot." Accessed on: October 6, 2019. Available from: https://snoflo.org/report/snow/alaska/coldfoot/history/

Stricker, J. (2015). "Dalton Highway Closure." *Alaska Business Monthly*: August 2015, 42-51.

Swann, K. (2015). "Expediting Cargo." *Alaska Business Monthly*: August 2015, 40-41.

Tang, H., Hu, X., Xu, C., Li, C., Yong, R. Wang, L. (2014). "A novel approach for determining landslide pushing force based on landslide-pile interactions." *Engineering Geology*: 182, 15-24, http://dx.doi.org/10.1016/j.enggeo.2014.07.024